frontiers | Frontiers in Earth Science

TYPE Original Research
PUBLISHED 11 December 2024
DOI 10.3389/feart.2024.1489700

OPEN ACCESS

EDITED BY
Saša Ahac,
University of Zagreb, Croatia

REVIEWED BY
Qidong Gao,
Chang'an University, China
Tanja Mališ,
University of Zagreb, Croatia
Mario Bacic,
University of Zagreb, Croatia

*CORRESPONDENCE
Kuangqin Xie,
2750525103@qq.com
Zonghao Yuan,
yuanzh@zjut.edu.cn

RECEIVED 01 September 2024
ACCEPTED 22 November 2024
PUBLISHED 11 December 2024

CITATION
Liang X, Xu J, Zhang Y, Zhou X, Xie K, Yuan Z, Zhang M, Wu J and Liu L (2024) Investigation into vibration propagation and attenuation characteristics of shield construction based on field measurement.
Front. Earth Sci. 12:1489700.
doi: 10.3389/feart.2024.1489700

Investigation into vibration propagation and attenuation characteristics of shield construction based on field measurement

Xu Liang[1], Jian Xu[1], Yapeng Zhang[2], Xuetao Zhou[2], Kuangqin Xie[3]*, Zonghao Yuan[3]*, Min Zhang[4], Jian Wu[5] and Long Liu[6]

[1]Hangzhou Urban Infrastructure Construction Management Center, Hangzhou, China, [2]Power China Huadong Engineering Corporation Limited, Hangzhou, China, [3]College of Civil Engineering, Zhejiang University of Technology, Hangzhou, China, [4]Institute of Transportation Engineering, Zhejiang University, Hangzhou, China, [5]The Zhejiang Engineering Research Center of Green Mine Technology and Intelligent Equipment, Hangzhou, China, [6]Zhejiang Huadong Engineering Construction and Management Corporation Limited, Hangzhou, China

Vibration caused by shield tunneling construction have adverse impacts on surrounding environment. To ascertain the influence of shield tunneling construction on ambient vibration, based on the shield tunnel project of Zhijiang Road in Hangzhou, the on-site vibration tests were carried out on the deep soil and surface during the excavation, and the vibration characteristics and vibration attenuation law during shield construction were investigated. The results show that the main frequency of vibration near the vibration source is wide, and the response components can be observed at 0–100 Hz. Under the filtering effect of the surface-covering soil layer, the high-frequency components of the vibration response are significantly attenuated, and the surface vibration is mainly distributed within 40 Hz. In the shield crossing, the deep measurement point is 5 dB higher than the vibration level of the same position on the surface. After the shield is pushed forward 20 m, the average attenuation of the surface vibration response is 10 dB, and the average attenuation of the deep vibration response is 12 dB.

KEYWORDS

shield construction, vibration response, field-test, attenuation law, deep vibration testing

1 Introduction

With the global acceleration of urban construction, the shield method has been widely adopted as an efficient and effective underground engineering construction method, and the consequent industrial vibration problems have become increasingly prominent. Vibration propagates outward through the surrounding strata, causing adverse effects on the structural safety of neighboring buildings, in particular leading to an irreversible negative impact on vibration-sensitive historic heritage buildings (Griefahn et al., 2006; Villot et al., 2013; Woodcock et al., 2013).

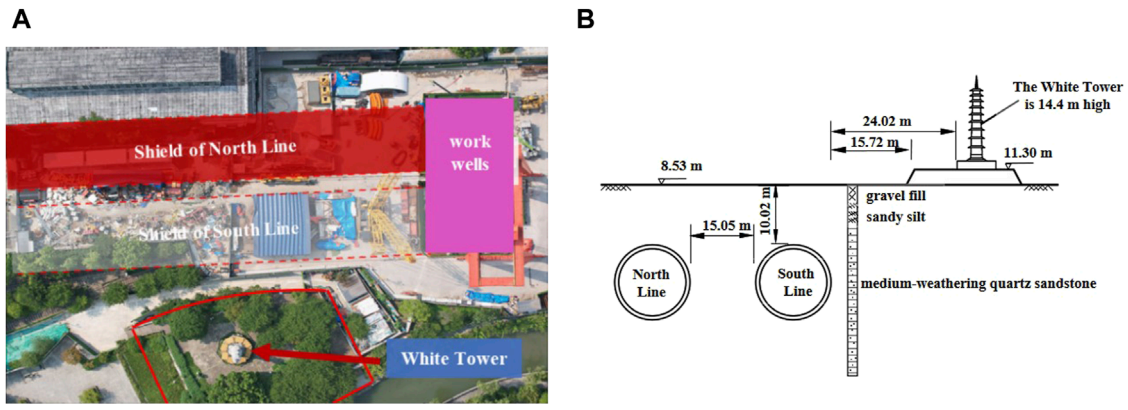

FIGURE 1
Location relationship between the shield and the White Tower. **(A)** Plane. **(B)** Section.

TABLE 1 Physical and mechanical parameters of the soil layer.

Name of soil layer	γ (kN/m^3)	E (MPa)	v	SV (m/s)	H (m)
gravel fill	19.3	4.0	0.35	164	1.5
sandy silt	20.7	20.0	0.22	329	1.1
medium-weathering quartz sandstone	26.0	—	0.29	473	—

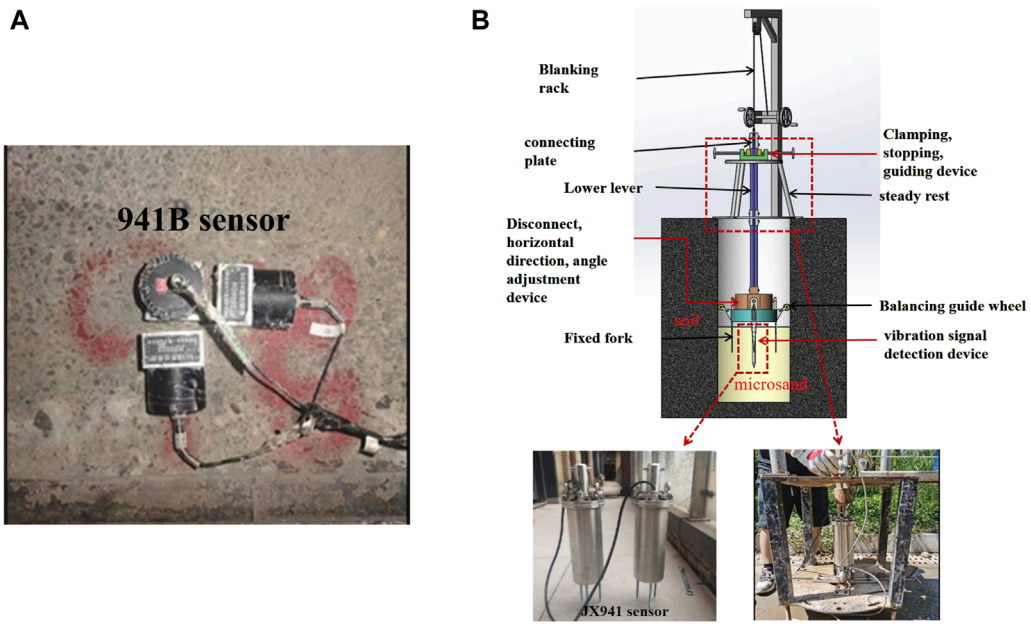

FIGURE 2
On-site vibration test. **(A)** Surface vibration testing. **(B)** Deep vibration testing.

Most current studies focus on the impact of long-term traffic vibration on buildings during tunnel operation (Liang et al., 2020; Fiala et al., 2007; Yuan et al., 2021; Hussein and Hunt, 2007). With the frequency of safety accidents in surrounding structures due to shield construction, several studies have focused on the environmental vibration caused by shield construction from three perspectives: the vibration source, vibration characteristics, and vibration propagation law. First, in terms of the vibration source, the results of the current study proved that the vibration sources in the shield construction process mainly include three

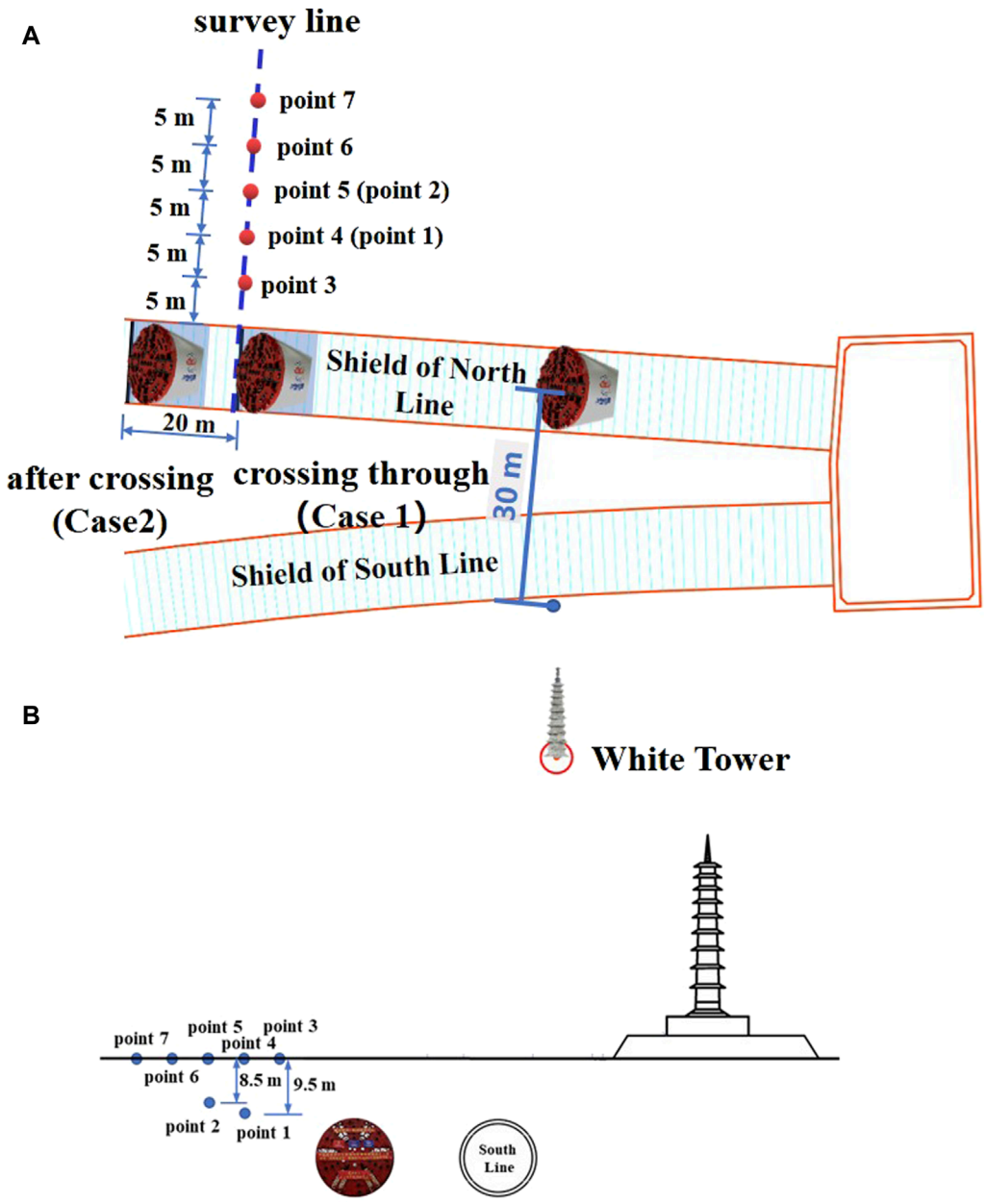

FIGURE 3
Vibration test scheme. **(A)** Plane. **(B)** Section.

categories: (a) vibration generated by the cutting tool cutting the soil during excavation; (b) vibration generated by the shield body operation; and (c) vibration generated by the construction supporting vehicle operation (Nelson et al., 1984; Hiller and Hope, 1998; Tao et al., 2015). Secondly, a significant amount of research has been conducted on vibration characteristics caused by shield construction. The vibration strength is directly related to the shield construction parameters and geological engineering conditions, among which the shield construction parameters include the total shield thrust, shield tunneling speed, cutter disc cutting torque, and rotational speed. Engineering geological parameters include the dynamic elastic modulus of the overburden, tunnel burial depth, etc., (Xu et al., 2021; Zhu et al., 2021). Sun et al. (2020) studied the frequency distribution of the single hob impact load response and found that the hob load frequency is mainly distributed in the range of 0–20 Hz, and the amplitude in the low-frequency range is positively correlated with the penetration degree, cutting speed, and the hardness of the rock layer. Through numerical simulation, Huo et al. (2015) found that the vibration frequency of the shield cutter plate is concentrated in the range of 0–20 Hz during the process of shield construction and the amplitude is greatly affected by the different geological conditions. Further, the vibration amplitude is greatly affected by different geological conditions. For sand and pebble strata, Guo et al. (2014) found that the frequency

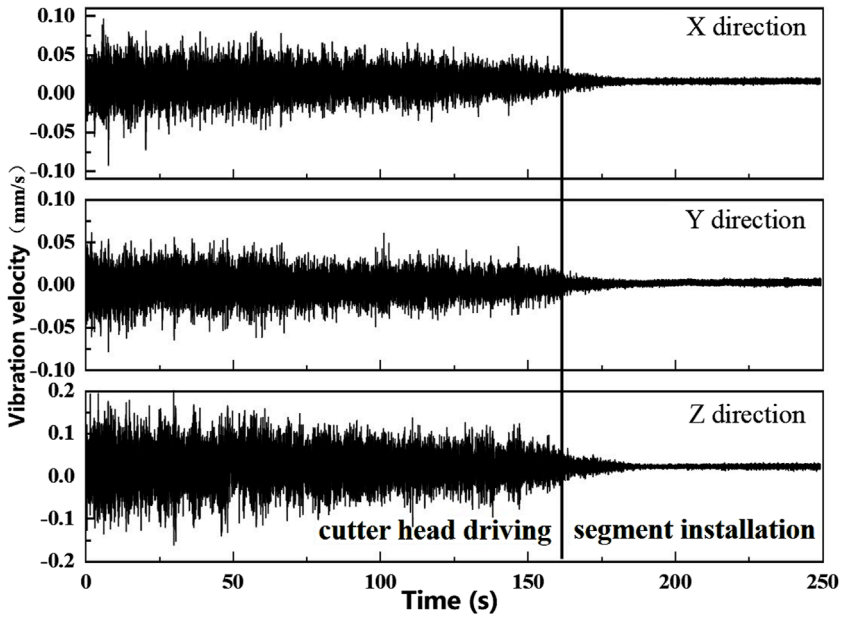

FIGURE 4
On-site testing of vibration at ground surface. The data are from the on-site monitoring daily reports: Zhijiang Road Water Pipeline Corridor and Road Upgrading Project Manager Department (2023).

band of vibration induced by the cutter plate digging is wider, and the main frequency is mainly concentrated in the range of 20–90 Hz, the frequency band of the amplitude of the rear supporting vehicle is 0–20 Hz, and the amplitude of the transportation vehicle is mainly concentrated in the range of 70–90 Hz. Lu (2023) studied the frequency distribution of vibration of the TBM construction in different stratigraphic layers, and the frequency distribution is 10–55 Hz in the soil fill layer, 25–64 Hz in the medium-coarse sand layer, and 20–64 Hz in the granite layer. Hong and Li (2022) carried out field tests on the shield section adjacent to the right and left pipes of the cutter plate during shield tunneling, finding that the vibration frequency bands were distributed in the range of 500 Hz, but were mainly concentrated in the range of 200 Hz or less. Finally, from the perspective of the vibration propagation law, Wu et al. (2022) predicted the dynamic response of the building structure under various building foundation types and horizontal distances from the tunnel by inputting the maximum acceleration obtained from the shield construction site into the tunnel–rock–building 3D finite element model. The results showed that the main impact distance of the segment vibration caused by rigid rock tunnel construction was approximately 9 m. Tao et al. (2015), Guo et al. (2018) investigated the characteristics of vibration sources through field measurements and numerical simulations for shield construction in the sandy gravel layer. Hong and Li (2022) found that the energy of vibration waves was mainly determined by the horizontal distance between the measurement point and the vibration source, and there was a vibration amplification zone within a certain distance from the center line of the shield tunnel through the field measurement of double-line shield construction in a sandy gravel stratum. The same phenomenon was found in Qin et al.'s study on the vibration response of a double-track tunnel, which they termed the "shadow effect" (Jin et al., 2020). Dai and Liu (2019) and Liao et al. (2009) carried out research on protection measures for under-passing vibration-sensitive buildings and implemented vibration control by adopting a series of technical means, such as the reasonable setting of shield parameters, muck improvement, axis control, vibration reduction of the horizontal transportation system, and automatic monitoring of the vibration effect. There are a large number of hobs on the cutter head and their distribution is complex. The formation parameters and tunneling parameters of the specific shield construction project are quite different, and the amplitude–frequency characteristics of the shield tunneling vibration source are quite different in the existing studies.

Vibration can cause irreversible damage to cultural relics and buildings; in the vibration impact assessment, not only should the threat of vibration be considered, but also the impact on integrity. In particular, for the vibration impact of cultural relics protection units, the "Technical specifications for protection of historic buildings against man made vibration" stipulates that the material fatigue limit is used as the control index of industrial vibration prevention of ancient buildings to achieve the purpose of protecting the structural integrity of ancient buildings. Among them, the national key cultural relics protection units allow strict vibration control indicators. When the elastic longitudinal wave of brick masonry is less than 1,600 m/s, the maximum horizontal vibration velocity at the highest point of the load-bearing structure should be controlled within 0.2 mm/s (GB/T 50452-2008, 2008). At present, the study of industrial vibration on ancient buildings at home and abroad is still in the initial stage, and the vibration source of shield tunneling in industrial vibration source is rarely mentioned, and related research is also relatively few. Herein, field measurements were carried out outside the White tower protection area of the Zhijiang Road water pipeline corridor, the deep layer and surface soil vibration testing were conducted, and the effects of shield

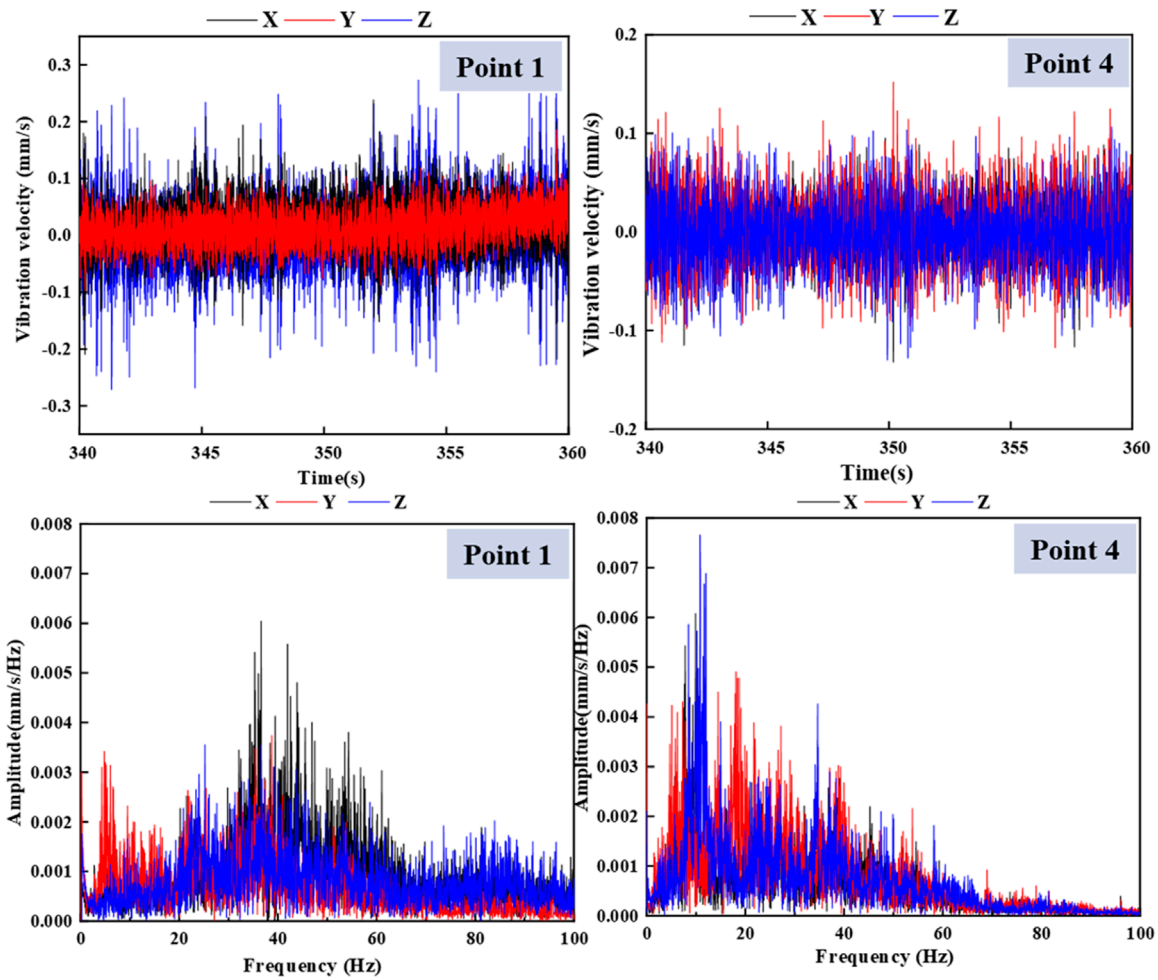

FIGURE 5
The time-frequency curves of typical measuring points under case 1.

tunneling construction on the vibration characteristics and vibration attenuation characteristics in the stratum were analyzed, which provides a reference for the construction and vibration control of the White tower in the near side of shield construction.

2 Field test scheme

2.1 Project background

The Zhijiang Road water pipeline corridor tunnel project has a total length of 3,246.7 m, of which the north line shield tunnel is 2,710 m, and the south line shield tunnel is 2,703 m. Both the south and north lines pass in vicinity of the White Tower, and the minimum horizontal distance between them and the White Tower is 24.02 m and 53.57 m, respectively. The buried depth of the tunnel is 10.02 m, and the net distance between the south and north lines is 15.05 m. The positional relationship between the White Tower and the tunnel is shown in Figure 1. The internal diameter of shield tunnel is 13.3 m, the external diameter is 14.5 m, and the tube pieces are 2 m per ring.

According to the drilling exposure and field wave velocity test, the stratum rocks within the depth of the shield tunnel can be divided into gravel fill, sandy silt, and medium-weathering quartz sandstone. The whole section of the shield tunneling is located in the medium-weathering quartz sandstone. The physical and mechanical property parameters of the soil layer are shown in Table 1. Among the parameters, H is the thickness of the soil layer, γ is natural gravity, E is the elastic modulus, v is the Poisson's ratio, and SV is the shear wave velocity.

2.2 Field test instruments and installation

During the field tests, the 941B ultra-low frequency vibration sensor was used for the surface measurement points, and the JX941 ultra-low frequency vibration sensor was used for the deep measurement points. The data acquisition instrument adopts an INV3060V network distributed acquisition instrument with a sampling frequency of 512 Hz and a monitoring and analysis frequency of 100 Hz. Among them, the JX941 ultra-low frequency vibration sensor needs to use supporting installation equipment.

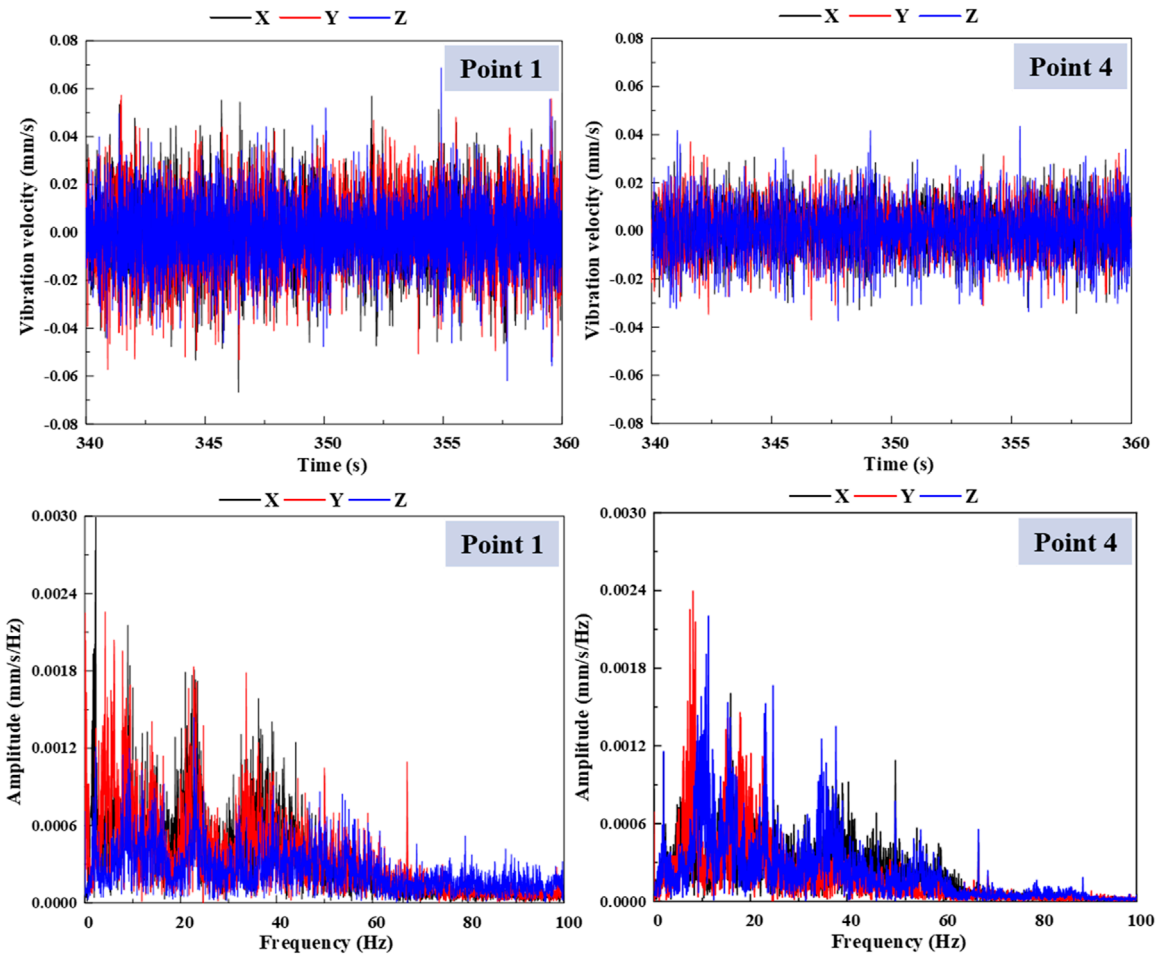

FIGURE 6
The time-frequency curves of typical measuring points under case 2.

The specific installation process is as follows: first, drill holes at the predetermined location on the ground surface until the specified depth, then install the landing gear at the hole location, and finally, lower the sensor along the hole to the selected area. The deep vibration testing instrument is mainly divided into three parts, namely, the clamping, stopping, and guiding device; the disengagement, horizontal, and angular adjustment device; and the vibration detection device. The vibration sensors are connected by fixed-length connecting rods through flange connectors, and put into the well in sequence, which can ensure the accurate depth of the sensors, and also help to ensure the accuracy of the test. Furthermore, the grouting pipe is fixed on the lowering rod and put into the well, which is convenient for grouting. Figure 2 shows the on-site vibration test.

Each measurement point tests the acceleration in three directions simultaneously, where the X direction is the shield-digging direction, the Y direction is perpendicular to the shield-digging direction, and the Z direction is the vertical direction. The test process and method are carried out according to the relevant provisions of the national standard reference (Chang, 2013; GB 10070-1988, 1988; GB 50911-2013, 2013).

2.3 Test scheme and working condition

This study aims to predict the characteristics of the vibration source and the attenuation law of vibration in the ground during shield tunneling and to study the impact of shield construction on the vibration response of the White Tower. In order to study the vibration response characteristics of the main construction steps in the shield construction process, vibration tests were carried out for cutter head driving and segment installation. Sensors were arranged at the surface position 30 m from the cross section of cutter head to the tunnel center and the plane position was shown in Figure 3A. Considering the vibration of the White Tower under the most dangerous working conditions, i.e., the south tunnel construction is directly on the side of the White Tower (at this time, the vibration source is 24 m away from the White Tower horizontally). During the construction of the north tunnel through the White Tower on the side, a vibration monitoring section was set up outside the White Tower's protection area, which includes five surface vibration measurement points and two deep vibration measurement points. In order to reduce the impact of the white tower in shield construction, two working conditions were considered in the field vibration tests

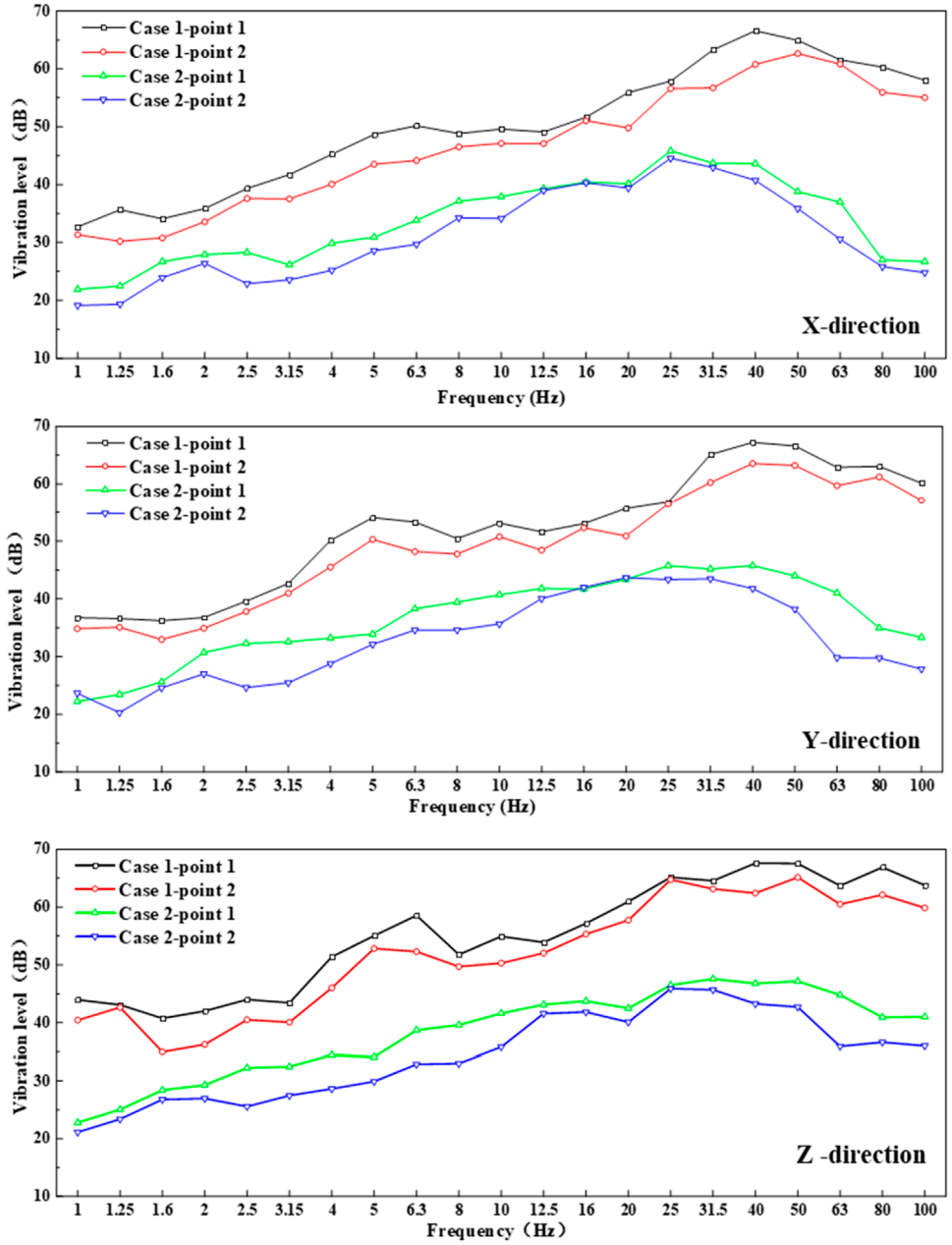

FIGURE 7
One-third octave curve of deep measuring point under various working conditions.

including crossing through (case 1) and after crossing (case 2), where the after-crossing condition is 20 m forward for the crossing-through condition. The vibration test scheme is shown in Figure 3.

3 Test results and discussion

3.1 Vibration source test

The surface vibration response caused by the main construction steps in the shield construction process is shown in Figure 4. According to the field vibration source test, when the cutter head is driving, the maximum vibration velocity in X, Y and Z direction of the surface vibration measurement point is 0.083, 0.059 and 0.198 mm/s, respectively. When the segment is assembled, the maximum vibration velocity in three directions is 0.019, 0.005 and 0.026 mm/s. The vibration velocity in X direction is greater than that in Y direction, and the vibration induced by cutter head driving is significantly greater than that of segment assembling. Therefore, cutter head driving is the main cause of surface vibration response.

3.2 Research on vibration characteristics

During the construction of shield tunneling, the coupling effect of various vibration sources makes the characteristics of vibration

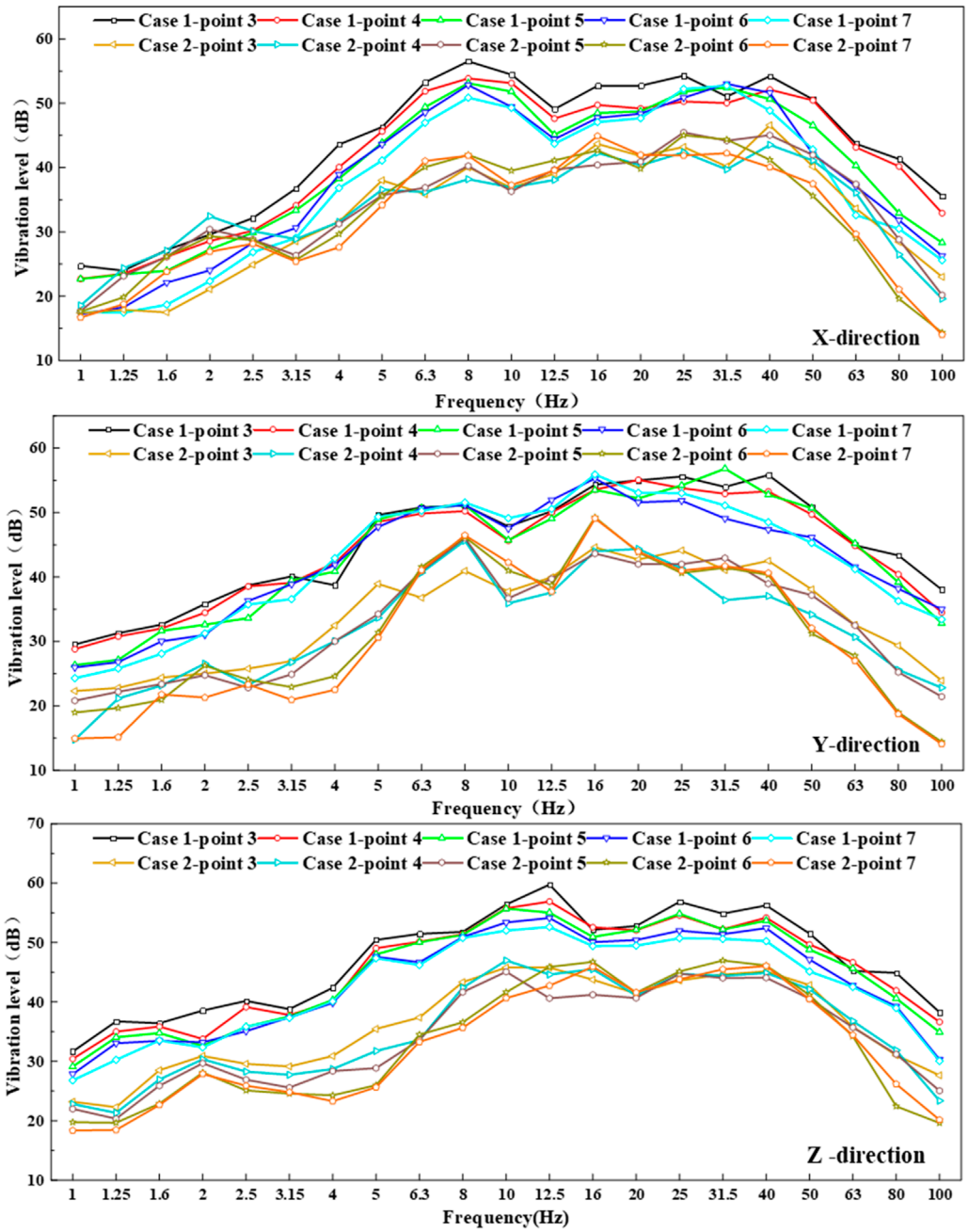

FIGURE 8
One-third octave curve of surface measurement points under different working conditions.

sources complex. Furthermore, the stratum parameters of construction projects and tunneling construction parameters are quite different, resulting in significant differences in the amplitude–frequency characteristics of shield tunneling vibrations. For this project, the vibration characteristics are studied. The time–frequency curves of typical measurement points are shown in Figures 5, 6.

From Figure 5, it can be seen that the three-way vibration of deep measurement points obviously differs during shield tunneling. The RMS vibration velocity in the X, Y, and Z directions are 0.046, 0.034, and 0.053 mm/s, respectively. The three-dimensional vibration response of the surface measurement points is close. The vibration response of the deep measurement point is significantly larger than that of the surface measurement point. In the same vertical direction, the vibration propagates from the deep measurement point to the surface measurement point, and the three-way vibration velocity effective value attenuation rates are 41%, 3%, and 38%, respectively. The vibration frequency band of deep measurement points caused by shield construction is wider than that of surface measurement points. Since Point 1 is located in the same soil layer as the shield palm surface (with a wave velocity of approximately 450 m/s) and is relatively close, the vibration characteristics are similar to those inside the shield machine: The frequency are

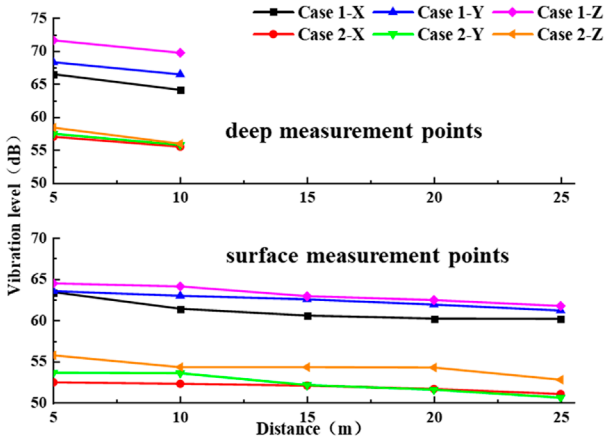

FIGURE 9
Curve of the total vibration level with increases in the horizontal distance.

distributed at 0–100 Hz, and the high-frequency components of 30–60 Hz are obvious. Under the filtering effect of the surface-covering soil layer, the high-frequency components of the vibration response are significantly attenuated, and the surface vibration is mainly distributed within 40 Hz.

It can be seen from Figure 6 that after the shield passes through, the three-way vibration responses of both the deep measurement points and the surface measurement points tend to be consistent. Among them, the RMS vibration velocity in the X, Y, and Z directions of the deep measurement points are 0.015, 0.014, and 0.011 mm/s, respectively. The RMS values of the X-direction, Y-direction, and Z-direction vibration velocities of the surface measurement points are 0.009, 0.009, and 0.010 mm/s, respectively. In the same vertical direction, the vibration propagates from the deep measurement point to the surface measurement point, and the effective value attenuation rates of the three-way vibration velocity are 40%, 36%, and 10%, respectively. When the shield is pushed forward 20 m, the attenuation rates of the three-dimensional vibration velocity of the deep measurement points are 69%, 59%, and 79%, respectively, and the attenuation rates of the three-dimensional vibration velocity of the surface measurement points are 67%, 73%, and 70% respectively. With the shield advancing forward, the frequency domain curve of the deep measurement point on the measuring line changes obviously, the high-frequency component attenuates significantly, and the vibration response is mainly distributed within 60 Hz.

3.3 One-third octave analysis

To reflect the vibration spectrum characteristics caused by shield tunneling in more detail, the frequency is divided into several frequency bands. In this paper, the one-third octave is used for spectrum analysis, and the vibration response intensity corresponding to different center frequencies is determined to evaluate the different frequencies of vibration. The one-third octave of each measurement point under different working conditions is shown in Figures 7, 8.

It can be seen from Figure 7 that when the shield is crossing through, in the 1–100 Hz frequency range concerned by the building, the vibration levels of the deep measurement points in the X, Y, and Z directions are 31–67, 32–68, and 34–68 dB, respectively. The one-third octave curve of vibration generally exhibits a trend of rising first and then falling, and the peak value of the high-frequency component greater than 40 Hz is obvious. When the vibration propagates from measurement point 1 to measurement point 2, the range of three-way vibration attenuation is 0–7, 0–6, and 0–7 dB, respectively, and the three-way vibration has a maximum attenuation at about 30–40 Hz. When the shield continues to advance 20 m, the three-way vibration levels of the deep measurement points decrease, and the ranges are 21–46, 22–46, and 22–48 dB, respectively. The peak value of the one-third octave curve of the vibration migrates to the low-frequency direction in comparison to case 1. When the vibration propagates from measurement point 1 to measurement point 2, the three-way vibration attenuation ranges are 0–5, 0–12, and 0–9 dB, respectively, and the three-way vibration has the maximum attenuation at 63 Hz. When the shield experiences different working conditions, the maximum attenuation of the three-way vibration level is 33, 31, and 26 dB, respectively. The maximum attenuation occurs in the high-frequency component of 63–100 Hz. When the shield is pushed forward by 20 m, the soil significantly filters the high-frequency component of the vibration.

It can be seen from Figure 8 that, when the shield crosses through, the vibration levels of the X, Y, and Z directions of the surface measurement points are in the range of 58, 56, and 60 dB, respectively. The three-way vibration is significantly attenuated in the part higher than 40 Hz than the deep measurement point, which is consistent with the conclusion obtained on the frequency domain diagram. The vibration level of the surface measurement point is higher in the low-frequency component, of 6–40 Hz. With increases in the horizontal distance from the vibration source, the vibration response exhibits a trend of attenuation overall, and the attenuation of the high-frequency component is also obvious. When the shield continues to advance 20 m, the three-way vibration levels of the surface measurement points decrease, and the deeper measurement points differ. When the shield advances forward, the surface measurement points attenuate significantly in the middle- and low-frequency bands. At this time, the vibration response of the five measurement points on the measurement point is more positive than the shield.

3.4 Attenuation law of the survey line section

To study the attenuation law of shield construction vibration in the stratum, the variation law of the three-way total vibration level and three-way effective vibration velocity with increases in the distance under different working conditions is studied. Figure 9 shows a curve of the total vibration level with increases in the horizontal distance under different working conditions.

From Figure 9, it can be seen that during the shield crossing, the three-way total vibration level range on the surface side line is 60–65 dB, and the three-way total vibration level range of the deep measurement point is 64–72 dB. The average vibration level of the deep measurement point is 5 dB higher than that of the same

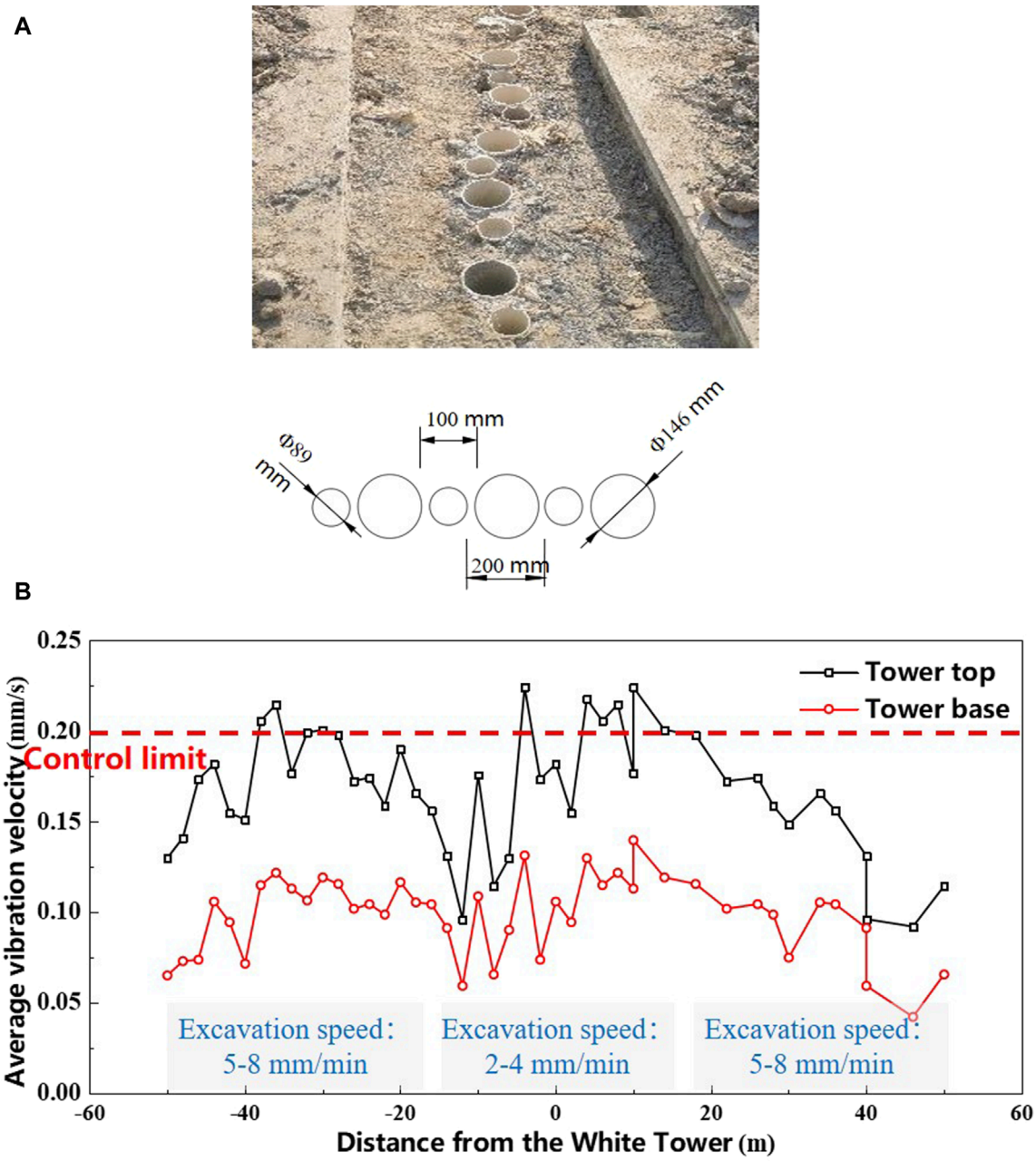

FIGURE 10
Safety control measures. **(A)** Vibration isolation boreholes. **(B)** Effectiveness of safety control measures. The data are from the on-site monitoring daily reports: Zhijiang Road Water Pipeline Corridor and Road Upgrading Project Manager Department (2023).

position on the surface, and the vibration response in the Z direction is greater than that in the Y direction and greater than that in the X direction, which is consistent with the conclusion of the time-domain diagram above. After shield crossing, the three-way total vibration level range on the surface survey line is 50–56 dB, and the three-way total vibration level range of the deep measurement point is 55–58 dB. The deep vibration is 3 dB higher than that of the surface. After the shield is pushed forward 20 m, the average attenuation of the surface vibration response is 10 dB, and the average attenuation of the deep vibration response is 12 dB. The vibration response in the Z direction is greater than that in the horizontal two-way direction. The effective vibration velocity is consistent with the law of the total vibration level.

3.5 Safety control measures

Based on the vibration characteristics and the vibration attenuation laws studied above, the final safety control measures for the White Tower are as follows: control the excavation speed to 2–8 mm/min, and install a row of 30-m-deep vibration isolation boreholes outside the White Tower. The dimensions of the isolation boreholes are detailed in Figure 10A. During the entire process of the

south line shield tunnel crossing, the maximum horizontal vibration response at the tower base was approximately 0.05–0.1 mm/s, and the maximum horizontal vibration response at the tower top was approximately 0.1–0.2 mm/s.

4 Conclusion

To solve the problems of complex vibration source characteristics and unclear vibration attenuation law in shield construction, based on the shield tunnel project of Zhijiang Road in Hangzhou, field tests of deep soil and surface vibration caused by shield tunneling are carried out to study the characteristics of the vibration source and the propagation law of the vibration in the stratum during the shield construction, the conclusions are as follows:

(1) Cutter head driving is the main cause of surface vibration response. The vibration frequency band of deep measurement points caused by shield construction are mainly distributed in 0–100 Hz, and the high-frequency components of 30–60 Hz are obvious. Under the filtering effect of the surface-covering soil layer, the high-frequency components of the vibration response are significantly attenuated, and the surface vibration is mainly distributed within 40 Hz.

(2) After the shield is pushed forward 20 m, the average attenuation of the surface vibration response is 10 dB, and the average attenuation of the deep vibration response is 12 dB.

(3) When the shield passes through, the three-dimensional vibration level range of the deep measurement point is 30–70 dB, and the one-third octave curve of the vibration generally exhibits a trend of rising first and then falling, and the peak value of the high-frequency component greater than 40 Hz is obvious. When the shield continues to advance 20 m, the average vibration level of the deep measurement point attenuates by 34 dB, and the maximum attenuation occurs at 63 Hz. When the shield passes through, the vibration level of the surface measurement point is within the range of 60 dB.

Data availability statement

The raw data supporting the conclusions of this article will be made available by the authors, without undue reservation.

Author contributions

XL: Writing–original draft, Data curation, Methodology. JX: Data curation, Investigation, Software, Writing–review and editing. YZ: Conceptualization, Investigation, Software, Writing–review and editing. XZ: Data curation, Methodology, Supervision, Writing–original draft. KX: Data curation, Formal Analysis, Methodology, Validation, Writing–original draft, Writing–review and editing. ZY: Conceptualization, Data curation, Formal Analysis, Funding acquisition, Investigation, Methodology, Project administration, Resources, Software, Supervision, Validation, Visualization, Writing–original draft, Writing–review and editing. MZ: Data curation, Formal Analysis, Project administration, Validation, Writing–original draft. JW: Formal Analysis, Project administration, Validation, Writing–review and editing. LL: Funding acquisition, Methodology, Project administration, Writing–original draft.

Funding

The author(s) declare that financial support was received for the research, authorship, and/or publication of this article. This work was supported by the National Natural Science Foundation of China (Grant nos. 52078462 and 52378376), Fundamental Research Funds for the Provincial Universities of Zhejiang (no. RF-B2023007), and Zhejiang Province Construction Research Projects (no. 2023K155).

Conflict of interest

Authors YZ and XZ were employed by Power China Huadong Engineering Corporation Limited. Author LL was employed by Zhejiang Huadong Engineering Construction and Management Corporation Limited.

The remaining authors declare that the research was conducted in the absence of any commercial or financial relationships that could be construed as a potential conflict of interest.

Publisher's note

References

Chang, H. Q. (2013). *Heritage impact assessment study of the Xi' an urban rail transit planning*. Xi' an, Shanxi, China: Xi' an University of Architecture and Technology.

Dai, Y. J., and Liu, T. (2019). Study on protection technology of metro shield tunneling under-passing vibration hypersensitive building. *Heilongjiang Jiaot.* 308, 139–142. doi:10.16402/j.cnki.issn1008-3383.2019.10.067

Fiala, P., Degrande, G., and Augusztinovicz, F. (2007). Numerical modelling of ground-borne noise and vibration in buildings due to surface rail traffic. *J. Sound Vib.* 301, 718–738. doi:10.1016/j.jsv.2006.10.019

GB 10070-1988 (1988). *Standard of vibration in urban area environment*.

GB 50911-2013 (2013). *Code of monitoring measurement of urban rail transit engineering*.

GB/T 50452-2008 (2008). *Technical specifications for protection of historic buildings against man made vibration*.

Griefahn, B., Marks, A., and Robens, S. (2006). Noise emitted from road, rail and air traffic and their effects on sleep. *J. Sound Vib.* 295, 129–140. doi:10.1016/j.jsv.2005.12.052

Guo, F., Huang, J., and Su, Y. (2014). Shield construction process induced vibration source characteristics. *J. Beijing Univ. Technol.* 40, 1820–1827.

Guo, F., Tao, L. J., and Kong, H. (2018). Analysis of propagation and attenuation of vibration induced by shield tunneling in Lanzhou sandy gravel layer. *Rock Soil Mech.* 39, 3377–3384. doi:10.16285/j.rsm.2016.2820

Hiller, D. M., and Hope, V. S. (1998). Ground borne vibration generated by mechanized construction activities. *Geotech. Eng.* 131, 223–232. doi:10.1680/igeng.1998.30714

Hong, Y., and Li, W. B. (2022). Dynamic effect induced by shield tunneling to existing tunnel. *J. Railw. Sci. Eng.* 19, 2005–2014. doi:10.19713/j.cnki.43-1423/u.t20210826

Huo, J., Wu, H., Yang, J., Sun, W., Li, G., and Sun, X. (2015). Multi-directional coupling dynamic characteristics analysis of TBM cutterhead system based on tunnelling field test. *J. Mech. Sci. Technol.* 29, 3043–3058. doi:10.1007/s12206-015-0701-1

Hussein, M. F. M., and Hunt, H. E. M. (2007). A numerical model for calculating vibration from a railway tunnel embedded in a full-space. *J. sound Vib.* 305, 401–431. doi:10.1016/j.jsv.2007.03.068

Jin, Q., Thompson, D. J., Lurcock, D., and Ntotsios, E. (2020). The shadow effect on the ground surface due to vibration transmission from a railway tunnel. *Transp. Geotech.* 23, 100335. doi:10.1016/j.trgeo.2020.100335

Liang, R., Liu, W., Ma, M., and Liu, W. (2020). An efficient model for predicting the train-induced ground-borne vibration and uncertainty quantification based on Bayesian neural network. *J. Sound Vib.* 495, 115908. doi:10.1016/j.jsv.2020.115908

Liao, S. M., Liu, J. H., Wang, R. L., and Li, Z. M. (2009). Shield tunneling and environment protection in Shanghai soft ground. *Tunn. Undergr. Space Technol.* 24, 454–465. doi:10.1016/j.tust.2008.12.005

Lu, Z. L. (2023). *Vibration influence law and prediction model of double-shield TBM construction in subway tunnel*. Qingdao, Shandong, China: Qingdao University of Technology.

Nelson, P. N., O'Rourke, T. D., and Flanagan, R. F. (1984). *Tunnel boring machine performance study*. Report No. 06-0100-84-1. Washington, DC: US Department of Transportation.

Sun, J. C., Liao, S. M., and Sun, L. Y. (2020). Analysis of impact load and vibration response of shield disc cuttersin soil-rock composite strata. *Mod. Tunn. Technol.* 57, 167–176. doi:10.13807/j.cnki.mtt.2020.05.021

Tao, L. J., Guo, F., and Huang, J. (2015). Field tests for environment vibration induced by shield tunneling in sand gravel layer. *J. Vib. Shock* 34, 213–218. doi:10.13465/j.cnki.jvs.2015.16.036

Villot, M., Bailhache, S., Guigou, C., and Jean, P. (2013). Prediction of railway induced vibration and ground borne noise exposure in building and associated annoyance. *Noise Vib. Mitig. Rail Transp. Syst.* 126, 289–296. doi:10.1007/978-3-662-44832-8_34

Woodcock, J., Peris, E., Waddington, D., and Moorhouse, A. T. (2013). Developing a good practice guide on the evaluation of human response to vibration from railways in residential environments. *Noise Vib. Mitig. Rail Transp. Syst.* 126, 305–312. doi:10.1007/978-3-662-44832-8_36

Wu, K., Zheng, Y., Li, S., Sun, J., Han, Y., and Hao, D. (2022). Vibration response law of existing buildings affected by subway tunnel boring machine excavation. *Tunn. Undergr. Space Technol.* 120, 104318. doi:10.1016/j.tust.2021.104318

Xu, R. Q., Guo, Z., and Ding, P. (2021). Overview on influence of vibration induced by shield construction on adjacent buildings and its control measures. *Tunn. Constr.* 41, 14–20.

Yuan, Z., Xu, D., Shi, L., Pan, X., Cai, Y., Hu, M., et al. (2021). Hybrid analytical-numerical modelling of ground vibrations from moving loads in a tunnel embedded in the saturated soil. *Eur. J. Environ. Civ. Eng.* 26, 6047–6075. doi:10.1080/19648189.2021.1928554

Zhijiang Road Water Pipeline Corridor and Road Upgrading Project Manager Department (2023). White tower ontology monitoring daily report . Hangzhou, Zhejiang: Civil Engineering Testing Center, Zhejiang University, 2022–2023 (in Chinese).

Zhu, J. C., Deng, Z. B., and Yuan, F. F. (2021). Investigation on main influencing factors on vibrations of tunnel boring machine in composite ground. *J. Zhejiang Univ. Technol.* 50, 435–443.